

# Binding of Hoechst 33258 to the TAR RNA of HIV-1. Recognition of a pyrimidine bulge-dependent structure

Laurent Dassonneville, François Hamy<sup>1</sup>, Pierre Colson<sup>2</sup>, Claude Houssier<sup>2</sup> and Christian Bailly\*

Laboratoire de Pharmacologie Moléculaire Antitumorale du Centre Oscar Lambret et INSERM Unité 124, Place de Verdun, 59045 Lille, France, <sup>1</sup>Pharma Research, Novartis Pharma Inc., CH-4002 Basle, Switzerland and <sup>2</sup>Laboratoire de Chimie Physique et Macromoléculaire, Université de Liège, 4000 Liège, Belgium

Received August 15, 1997; Revised and Accepted September 18, 1997

## ABSTRACT

The transactivation response region (TAR) RNA is an essential component in transcriptional regulation of the human immunodeficiency virus type-1 (HIV-1) genome. We have examined the interaction between TAR RNA and the bisbenzimidazole derivative Hoechst 33258. Previous studies have shown that this drug, which is well known as an AT-selective DNA minor groove binder, can also interact with GC-rich sequences in DNA as well as with RNA, possibly by intercalation. Absorption spectroscopy, circular dichroism and electric linear dichroism, as well as RNase A footprinting, were employed to compare binding of Hoechst 33258 to wild-type RNA and its analogue lacking the pyrimidine bulge. The uridine bulge, which is an important contributor to the structural stability of TAR, plays an essential role in drug binding. Deletion of the bulge destabilizes both free and drug-bound forms of TAR and markedly affects the orientation of the drug chromophore complexed with the RNA. According to the linear dichroism data, the bisbenzimidazole is oriented more or less perpendicular to the RNA helix axis. The data are compatible with a model in which the bisbenzimidazole chromophore is inserted into the existing cavity created by the pyrimidine bulge. The footprinting experiments, showing that the drug binds to a unique site opposite the unpaired uridine residues, also support this model. The binding of Hoechst 33258 to the sequence 5'-GCUCU, which delimits the cavity, reflects the greater accessibility of that region compared with other sites in the RNA molecule. The identification of a binding site for small molecules in TAR offers promising perspectives for developing drugs that would block the access of TAR RNA to proteins and therefore for the design of anti-HIV agents.

## INTRODUCTION

All nascent HIV-1 transcripts contain at their 5'-end the transactivation responsive (TAR) RNA element, a 59 base

stem-bulge structure capped by a hexanucleotide loop (Fig. 1), which binds to the *tat* protein (1). The *tat*-TAR interaction causes a substantial increase in transcript level, which may result from preventing premature termination of the transcriptional elongation complex (2). Deletion studies have shown that the region from +19 to +42 incorporates the minimal domain that is both necessary and sufficient for *tat* responsiveness *in vivo* (3). Within this minimal domain the apical 6 nt loop and the 3 nt pyrimidine bulge, which separates two helical stem regions, are both essential for transactivation. The loop is required for *in vivo* transactivation but is not involved in *tat* binding, which occurs specifically at the trinucleotide bulge (4). NMR studies have shown that the bulge and the adjacent base pairs recognized by the protein are found in an exceptionally wide and accessible major groove (5,6). Binding of *tat* results in a profound conformational change characterized by a significant compression of the protein binding pocket at the pyrimidine bulge (6,7).

Small molecules targeting the open (*tat*-free) or closed (*tat*-bound) protein binding site could antagonize the transactivation response and therefore may exhibit HIV-specific antiviral activity. In recent years attempts to identify specific inhibitors of the *tat*-TAR interaction have been initiated (reviewed in 8). Very recently the first compound able to inhibit *tat*-TAR interaction *in vitro* and *in vivo* was reported. This compound was selected from a peptoid combinatorial library of >3 000 000 compounds and effectively suppresses HIV-1 replication (9). This pioneer study not only validates the concept that a low molecular weight compound can be designed to specifically block *tat*-TAR interactions in human lymphocytes but also sets the stage for the design of anti-HIV-1 drugs. It is therefore of primary importance to better understand whether and how small molecules can bind to TAR RNA.

We have previously shown that classical DNA intercalating agents, such as proflavine and ethidium, can also intercalate into TAR RNA and that drugs usually referred to as AT-specific DNA minor groove binders, such as Hoechst 33258 and DAPI, bind to TAR RNA via a non-classical intercalation process similar to their mode of binding to GC-rich regions of double-stranded DNA (10). In the present study we have extended our investigation on binding of the bisbenzimidazole derivative Hoechst 33258 (also called pibenzimol) to wild-type TAR RNA and a deletion mutant lacking the pyrimidine bulge (Fig. 1). It has been previously

\*To whom correspondence should be addressed. Tel: +33 3 20 16 92 18; Fax: +33 3 20 16 92 29; Email: bailly@lille.inserm.fr

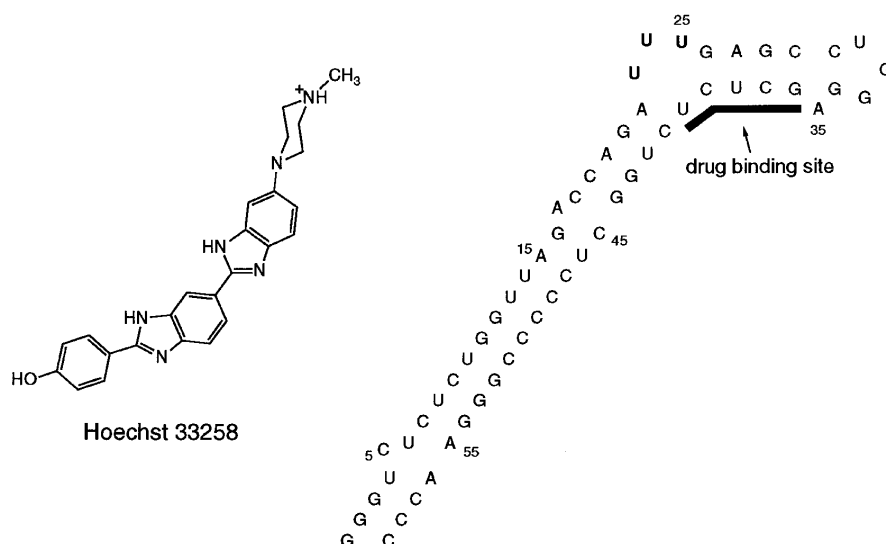


**Figure 1.** Structure of Hoechst 33258 and TAR RNA. The uridine bulge (in bold) is missing in  $\Delta$ U-TAR RNA. The position of the drug binding site inferred from the footprinting experiments is indicated.

shown that Hoechst 33258 has significant interaction with poly(A)-poly(U) (11) and that bisbenzimidazoles, including Hoechst 33258, bind tightly to a unique site in tRNA (12). This information and our previous works on the sequence-dependent binding modes of Hoechst 33258 to DNA (13) have prompted us to use this drug as a model ligand to study the interaction between small molecules and RNA.

## MATERIALS AND METHODS

### Drugs

Hoechst 33258 [2'-(4-hydroxyphenyl)-5-(4-methyl-1-piperazinyl)-2,5'-bis-1*H*-bisbenzimidazole], DAPI (4',6-diamidino-2-phenylindole) and distamycin were purchased from Sigma Chemical Co. Ligand concentrations were determined spectroscopically in 10 mm path length quartz cuvettes using the molar extinction coefficients (per M/cm): 35 000 at 302 nm for distamycin; 42 000 at 338 nm for Hoechst 33258; 27 000 at 342 nm for DAPI. All other chemicals were analytical grade reagents and solutions were prepared with double distilled sterile water to prevent nuclease contamination. Tubes and tips were treated with 1% diethylpyrocarbonate (DEPC; Sigma).

### *In vitro* transcription of TAR and $\Delta$ U-TAR RNA

Synthetic oligonucleotides corresponding to wild-type TAR and  $\Delta$ U-TAR sequences were cloned between *Hind*III and *Eco*RI sites of plasmid pUC19. After digestion with *Eco*RI the RNA was transcribed as a run-off product of 60 (TAR) and 57 ( $\Delta$ U-TAR) nt from the T3 RNA polymerase promoter. In each case the transcript includes an additional G residue on the 3'-end derived from the *Eco*RI cleavage site. The transcription reaction was performed in buffer containing 40 mM Tris-HCl, pH 7.4, 25 mM NaCl, 16 mM MgCl<sub>2</sub>, 10 mM DTT and 1 mM NTPs. The reaction was initiated by addition of 10  $\mu$ g linearized plasmid DNA template and 40  $\mu$ g T3 RNA polymerase and incubated for 2 h at 37°C. Nucleic acids were then fractionated on a 10% (w/v) polyacrylamide gel containing 8 M urea in TBE buffer (89 mM

Tris-borate, pH 8.3, 10 mM EDTA). After electrophoresis the RNA was eluted in water for 18 h at 4°C and precipitated with ethanol. The RNA was resuspended in water to give a 500  $\mu$ M stock solution ( $\epsilon_{260}$ /phosphate = 10 688/M/cm). For the footprinting experiments the RNA was 3'-end-labelled with [<sup>32</sup>P]cytidine biphosphate and T4 RNA ligase and then repurified from a 10% denaturing acrylamide gel (2).

### Absorption spectroscopy and melting temperature studies

Absorption spectra were recorded on a Uvikon 943 spectrophotometer. The 12-cell holder was thermostated with a Neslab RTE 111 cryostat. Drug-RNA complexes were prepared by adding aliquots of a concentrated Hoechst 33258 solution to a RNA solution at constant concentration (usually 20  $\mu$ M) in BPE buffer (6 mM Na<sub>2</sub>HPO<sub>4</sub>, 2 mM Na<sub>2</sub>H<sub>2</sub>PO<sub>4</sub>, 1 mM EDTA, pH 7.1). A heating rate of 1°C/min was used and data points were collected every 30 s. The temperature inside the cuvette was monitored by using a thermocouple. The absorbance at 260 nm was measured over the range 25–90°C in 1 cm path length reduced volume quartz cells. The 'melting' temperature  $T_m$  was taken as the midpoint of the hyperchromic transition determined from first derivative plots. The reproducibility of the  $T_m$  measurements was  $\pm 1$ °C.

### Circular dichroism (CD)

Measurements were recorded on a Jobin-Yvon CD6 dichrograph interfaced to a PC microcomputer. Solutions of drugs and/or RNA were scanned in 1 cm quartz cuvettes. Five scans were accumulated and averaged automatically. Spectra were recorded from 450 to 200 nm in 1 mM sodium cacodylate buffer adjusted to pH 6.5 at room temperature (20°C).

### Electric linear dichroism (ELD)

The procedures previously outlined were followed (10). The TAR RNA molecules were oriented by an electric pulse and dichroism in the region of the absorption bands of the RNA or of the ligand bound to RNA was probed using linearly polarized light.

**Table 1.** Spectral characteristics of drug–RNA complexes

Drug	$\lambda_{\max}^{\text{free}}$ (nm)	TAR RNA			$\Delta$ U-TAR RNA		
		$\lambda_{\max}^{\text{bound}}$ (nm)	$\Delta\lambda^a$ (nm)	Hypochromism (%)	$\lambda_{\max}^{\text{bound}}$ (nm)	$\Delta\lambda^a$ (nm)	Hypochromism (%)
Distamycin	303.3	303.8	0.5	0	303.5	0.2	0
Hoechst	337.7	348.5	10.8	46	344.8	7.1	35
DAPI	342.9	353.3	10.4	32	348.8	5.9	14

<sup>a</sup>Bathochromic shift ( $\lambda_{\max}^{\text{bound}} - \lambda_{\max}^{\text{free}}$ ).

### RNase A footprinting, gel electrophoresis and data processing

The procedure for the footprinting experiments was adapted from published protocols (14). Briefly, samples of the labelled RNA fragment were incubated with a buffered solution containing the desired drug concentration. After 20 min incubation at 4°C to ensure equilibration, digestion was initiated by addition of the RNase A solution. After 1 min incubation at room temperature the reaction was stopped by freeze drying and samples were lyophilized. The RNA in each tube was resuspended in 5  $\mu$ l formamide–TBE loading buffer, denatured at 90°C for 4 min, then chilled in ice for 4 min prior to loading onto a 0.3 mm thick, 10% polyacrylamide gel containing 8 M urea and TBE buffer (89 mM Tris base, 89 mM boric acid, 2.5 mM Na<sub>2</sub>EDTA, pH 8.3). After 2 h electrophoresis at 1500 V the gel was soaked in 10% acetic acid for 10 min, transferred to Whatman 3MM paper, dried under vacuum at 80°C and then analyzed in a phosphorimager (Molecular Dynamics). Each resolved band on the autoradiograph was assigned to a particular bond within the RNA fragment by comparison of its position relative to sequencing standards generated by treatment of the RNA with diethylpyrocarbonate followed by aniline-induced cleavage at the modified bases (A track).

## RESULTS

### Absorption studies

Figure 2 displays the spectral changes that occur when the TAR RNA or the  $\Delta$ U-TAR RNA is added to a solution of Hoechst 33258. In both cases a marked bathochromic shift and hypochromism are observed. The spectral modifications are larger with the wild-type RNA than with the mutant lacking the uridine bulge. The spectral characteristics measured with Hoechst 33258 and two other drugs, DAPI and distamycin, are reported in Table 1. All three drugs are known to bind to the minor groove of DNA and exhibit a sharp preference for AT-rich sequences (15). However, only Hoechst 33258 and DAPI can also interact with GC-rich sequences, possibly by intercalation (13,16–18). As indicated, the interaction of DAPI and Hoechst 33258 with TAR RNA causes a displacement in the absorption maximum of 10 nm and a large hypochromism (>30%) owing to perturbation of the complexed chromophore system on binding to RNA. No such effect was observed with distamycin, which apparently fails to bind to the RNA.

The hypochromism is more pronounced with Hoechst 33258 than with DAPI and for both drugs the shifts are larger with TAR than with  $\Delta$ U-TAR, suggesting that the two drugs interact more strongly with the former than with the latter RNA. It is already obvious at this stage that Hoechst 33258 interacts strongly with the highly structured TAR RNA.

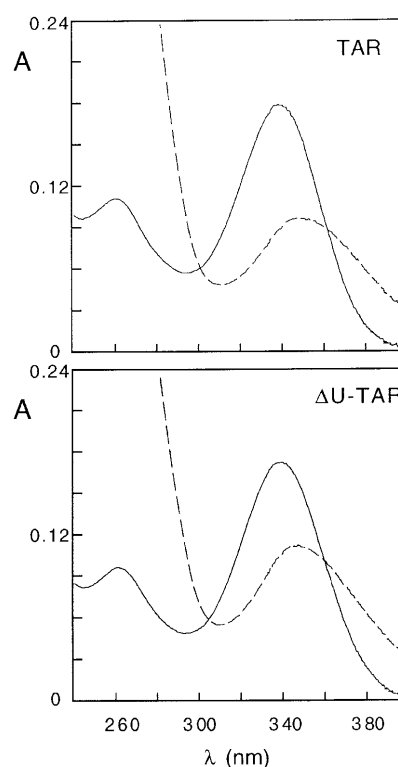


**Figure 2.** Absorption spectra of Hoechst 33258 (5  $\mu$ M) in the absence (solid line) and presence (dashed line) of RNA (20  $\mu$ M). The spectral parameters are given in Table 1.

### Thermal denaturation

The ability of Hoechst 33258 to alter the thermal denaturation profile of the RNA can also be used as another indication of its propensity to bind to TAR. The melting profiles of TAR and  $\Delta$ U-TAR in the absence and presence of the drug are shown in Figure 3. In each case simple monophasic melting curves were obtained. The helix-to-coil transition is sharp with the TAR RNA, whereas it is not so well defined with the bulge-less analogue. The gradual increase in absorbance over a broad temperature range suggests that the  $\Delta$ U-TAR RNA contains regions of differing stabilities. The melting temperature ( $T_m$ ) is 4–5°C lower with  $\Delta$ U-TAR than with TAR, indicating that the native RNA is notably more stable than the mutant. The bulge contributes to stabilization of the folded conformation. A large increase in the  $T_m$  of both TAR and  $\Delta$ U-TAR is observed in the presence of Hoechst 33258. The hyperchromicity is higher for the sample treated with Hoechst because there is a significant contribution of absorbance by the ligand at 260 nm. The  $\Delta T_m$  ( $T_m$  of the

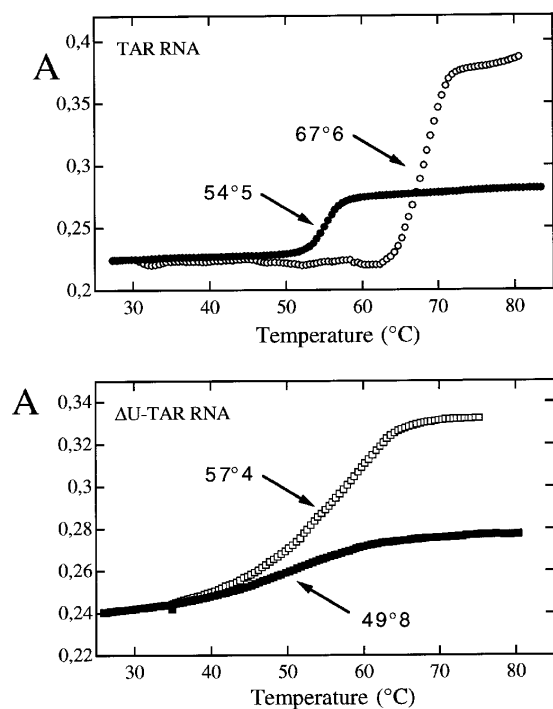


**Figure 3.** Thermal denaturation curves for (top) TAR and (bottom)  $\Delta$ U-TAR (20  $\mu$ M each) in the absence (filled symbols) and presence (open symbols) of 20  $\mu$ M Hoechst 33258. The indicated  $T_m$  values ( $^{\circ}$ C) were obtained from first derivative plots.

drug–RNA complex –  $T_m$  of the free RNA) is 13.1 and 7.6 $^{\circ}$ C with TAR and  $\Delta$ U-TAR respectively. Therefore, the  $\Delta T_m$  drops by nearly half when the uridine bulge is removed. This test provides another independent indication of the preferred binding of Hoechst 33258 to TAR compared with  $\Delta$ U-TAR. No change in the  $T_m$  was observed with distamycin, consistent with the lack of binding of this drug to the RNA. The stabilizing action of DAPI is only slightly lower than that of Hoechst 33258 (data not shown).

### Circular dichroism

The CD spectra of TAR and  $\Delta$ U-TAR in the absence of drug are slightly different (not shown). The spectrum of TAR displays a weak negative band at 235 nm adjacent to a large positive band centered at 265 nm, characteristics of an A-form helix. The spectrum of  $\Delta$ U-TAR is less well defined and the intensity of the positive band at 270 nm is much weaker than that of TAR. This suggests that  $\Delta$ U-TAR does not adopt a highly ordered structure, though it is nevertheless folded into an A-type conformation. The CD spectra concur with the melting profiles that the uridine bulge is an essential feature of the TAR RNA structure.

To examine the drug interaction we recorded the CD spectra in the 300–450 nm region. In the absence of RNA the Hoechst spectrum shows a weak positive CD centered at 350 nm. In the presence of the RNA the CD at 350 nm decreases rapidly to become negative and a new positive band appears at 380 nm. As shown in Figure 4, the amplitude of the positive band at 380 nm is virtually identical for the complexes of Hoechst 33258 with TAR and  $\Delta$ U-TAR. In contrast, the decrease in the CD at 340 nm is much more pronounced with TAR than with  $\Delta$ U-TAR (for identical drug–RNA ratios). In both cases binding appears geometrically

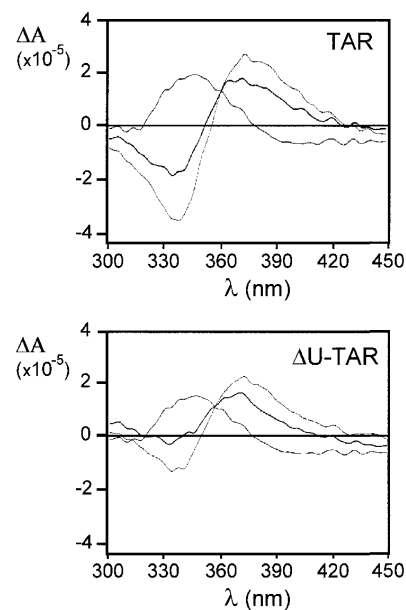


**Figure 4.** Circular dichroism of Hoechst 33258 (5  $\mu$ M) in the absence and presence of TAR and  $\Delta$ U-TAR. In the two panels the RNA phosphate/drug ratio (P/D) is 0, 2 and 4 (top to bottom curves at 340 nm). Measurements were made by progressive addition of RNA to the ligand solution of constant concentration in order to obtain the desired drug/DNA ratio.

homogeneous, as judged from the presence of an isodichroic point at 360 and 357 nm with TAR and  $\Delta$ U-TAR respectively.

### Electric linear dichroism

The ELD spectra of Hoechst bound to TAR and  $\Delta$ U-TAR (Fig. 5) reinforce the conclusion that interaction with the native structure is privileged over binding to the mutant RNA, since the reduced dichroism at 320 nm is much more negative with TAR than with  $\Delta$ U-TAR. The amplitude of the ELD signals in the drug absorption band is not only identical to that obtained with TAR RNA alone ( $\Delta A/A = -0.12$ ) but is also very similar to that measured with classical intercalating drugs such as proflavine and ethidium bromide. The ELD data with TAR are reminiscent of those reported recently with a series of drugs including both classical and DNA-threading intercalating agents (10) and therefore suggest, at first sight, that Hoechst 33258 forms stable intercalation complexes with TAR RNA. The ELD experiments were also performed with distamycin, but only very weak signals could be detected in the presence of TAR or  $\Delta$ U-TAR.

### Footprinting

As an attempt to identify a potential Hoechst 33258 binding site on TAR RNA, we probed the RNA and RNA–drug complexes with RNase A. Since the susceptibility of RNA to attack by RNase A is dependent on secondary structure rather than on primary sequence, this enzyme is not the most appropriate nuclease to monitor drug binding to the two double-stranded stem regions of the RNA. However, this enzyme is particularly well suited for investigating drug binding to the single strand parts, including the bulge and loop regions. The cleavage patterns are shown in Figure 6. The strong cleavage at positions 36–40 is largely reduced in the presence of the drug. In contrast, the cutting



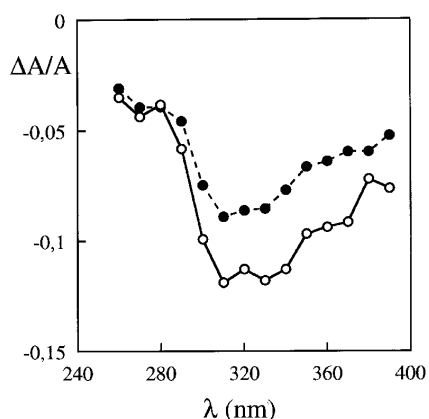


**Figure 5.** Electric linear dichroism spectra of Hoechst 33258 bound to (○) TAR and (●)  $\Delta$ U-TAR RNA. The reduced dichroism ( $\Delta A/A$ ) was measured in the presence of 50  $\mu$ M RNA and 10  $\mu$ M Hoechst 33258 (P/D = 5) in 1 mM sodium cacodylate buffer, pH 6.5, under a field strength of 13 kV/cm.

rate is increased significantly at other nucleotide positions, such as at G32 and C45. The reactivity of the nucleotide residues near the apical loop (positions 23–25) is apparently not affected by drug binding. The extent of protection at the 5'-GCUCU site (positions 36–40) as well as the enhanced cleavage at C45 is directly proportional to drug concentration. RNase A is detecting a concerted change in the helix conformation as a result of specific binding of Hoechst to the GCUCU site. We are inclined to interpret the base protection effects as being due to direct interaction with the ligand, but we cannot exclude the possibility that the protection arises from drug-induced structural changes. Protection caused by drug-dependent conformational changes that result in formation of a RNase A-resistant local structure cannot be readily distinguished from those caused by direct ligand–RNA contacts. However, on the basis of relaxation measurements indicating that the structure of the RNA is not markedly changed upon drug binding, we can confidently consider that the footprint arises from a direct drug–RNA interaction. The same footprint at the GCUCU site was detected using copper–phenanthroline as the cleaving agent.

Footprinting experiments were also performed with  $\Delta$ U-TAR, but no changes in the digestion pattern were observed in the presence of Hoechst 33258, even when using drug concentrations as high as 100  $\mu$ M (gel not shown). This suggests that the drug does not bind to any specific site in the bulge-deleted RNA. However, it must be mentioned that because of removal of the bulge, the double-stranded sequence at position 36–40 is now cut poorly by RNase A and therefore it is difficult to monitor potential drug binding to this sequence.

## DISCUSSION

In contrast to the DNA minor groove binder distamycin, Hoechst 33258 binds tightly to TAR and adopts a well-defined geometry. The TAR structure is strongly stabilized when Hoechst binds to it. Also, the 3 nt bulge that is crucial for interaction with *tat* protein and other cellular factors (e.g. the bulge binding protein) (19) is also important for drug binding.

A knowledge of the structure of TAR RNA in the absence and presence of ligands (5,6) offers a structural basis to rationalize our

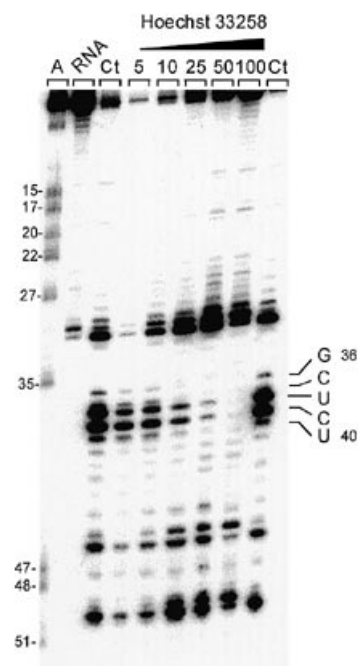


**Figure 6.** RNase A footprinting of Hoechst 33258 on TAR RNA. The RNA was 3'-end-labelled with [ $^{32}$ P]cytidine biphosphate and T4 RNA ligase. The cleavage products of the RNase A digestion were resolved on a 10% polyacrylamide gel containing 8 M urea. The concentration ( $\mu$ M) of the drug is shown at the top of the appropriate gel lanes. The control track labelled Ct contained no drug. The track labelled A represents diethylpyrocarbonate–aniline markers specific for adenines. Numbers on the left side of the gel refer to the numbering scheme used in Figure 1.

data. According to NMR, in free TAR RNA the bulged U23 residue is stacked within the helix, whereas the U25 residue is looped out. This arrangement creates a major distortion of the phosphate backbone and defines a pocket of major groove accessibility surrounding the bulge. The stacking interactions between the bases U40 and C39, i.e. precisely where Hoechst 33258 binds, are weak (6). It is therefore plausible that Hoechst 33258 exploits this intrinsic weakness to insert its chromophore at that particular site. The cavity formed by folding of the bulge provides a privileged binding site for Hoechst 33258, but also for other ligands. Indeed, the sequence at positions 38–40 is strongly cleaved by phenanthroline–copper complexes and is protected from cleavage upon binding of *tat*-related peptides (20). There is good reason to believe that different types of drugs can fit neatly into this existing cavity, which in some way may be viewed as the Achilles heel of TAR RNA. Bulges in RNA are usually good sites for drugs and for intercalators in particular. Ten years ago it was shown that small bulges in RNA hairpins enhance intercalation of ethidium bromide and promote an allosteric transition (21,22). More recently it was reported that the enediyne drug dynemicin, which also possesses an intercalating chromophore, can cleave RNA at single-stranded loop regions (23). Therefore, the present results showing that Hoechst 33258 is positioned near or possibly in contact with the pyrimidine bulge of TAR are consistent with the literature data and offer promising perspectives for developing drugs that would block the access of TAR RNA to proteins. Hoechst 33258 may warrant particular attention as a starting point for the design of new potential anti-HIV drugs.

## ACKNOWLEDGEMENTS

This work was supported by research grants (to C.B.) from the Agence Nationale de la Recherche sur le SIDA (ANRS), (to C.H. and P.C.) from Actions de Recherches Concertées contract 95/00-93 and the FNRS, Télévie 7/4526/96. Support by the 'convention INSERM-CFB' is acknowledged.

## REFERENCES

- 1 Gait,M.J. and Karn,J. (1993) *Trends Biochem. Sci.*, **18**, 255–259.
- 2 Churcher,M.J., Lamont,C., Hamy,F., Dingwall,C., Green,S.M., Lowe,A.D., Butler,P.J.G., Gait,M.J. and Karn,J. (1993) *J. Mol. Biol.*, **230**, 90–110.
- 3 Selby,M.J., Bain,E.S., Luciw,P.A. and Peterlin,B.M. (1989) *Genes Dev.*, **3**, 547–558.
- 4 Dingwall,C., Ernberg,I., Gait,M.J., Green,S.M., Heaphy,S., Karn,J., Lowe,A.D., Singh,M. and Skinner,M.A. (1990) *EMBO J.*, **9**, 4145–4153.
- 5 Aboul-ela,F., Karn,J. and Varani,G. (1995) *J. Mol. Biol.*, **253**, 313–332.
- 6 Aboul-ela,F., Karn,J. and Varani,G. (1996) *Nucleic Acids Res.*, **24**, 3974–3981.
- 7 Wang,Z. and Rana,T.M. (1996) *Biochemistry*, **35**, 6491–6499.
- 8 Chow,C.S. and Bogdan,F.M. (1997) *Chem. Rev.*, **97**, 1489–1513.
- 9 Hamy,F., Felder,E.R., Heizmann,G., Lazdins,J., Aboul-ela,F., Varani,G., Karn,J. and Klimkait,T. (1997) *Proc. Natl. Acad. Sci. USA*, **94**, 3548–3553.
- 10 Bailly,C., Colson,P., Houssier,C. and Hamy,F. (1996) *Nucleic Acids Res.*, **24**, 1460–1464.
- 11 Wilson,W.D., Ratmeyer,L., Zhao,M., Strekowski,L. and Boykin,D.W. (1993) *Biochemistry*, **32**, 1098–1104.
- 12 Ebrahimi,S.E.S., Wilton,A.N. and Douglas,K.T. (1996) *J. Chem. Soc. Chem. Commun.*, 385–386.
- 13 Bailly,C., Colson,P., Hénichart,J.P. and Houssier,C. (1993) *Nucleic Acids Res.*, **21**, 3705–3709.
- 14 Weeks,K.M. and Crothers,D.M. (1991) *Cell*, **66**, 577–588.
- 15 Portugal,J. and Waring,M.J. (1987) *Eur. J. Biochem.*, **167**, 281–289.
- 16 Wilson,W.D., Tanius,F.A., Barton,H.J., Strekowski,L. and Boykin,D.W. (1989) *J. Am. Chem. Soc.*, **111**, 5008–5010.
- 17 Tanius,F.A., Veal,J.M., Buczak,H., Ratmeyer,L.S. and Wilson,W.D. (1992) *Biochemistry*, **31**, 3103–3112.
- 18 Moon,J.-H., Kim,S.K., Sehlstedt,U., Rodger,A. and Nordén,B. (1996) *Biopolymers*, **38**, 593–606.
- 19 Baker,B., Muckenthaler,M., Vives,E., Blanchard,A., Braddock,M., Nacken,W., Kingsman,A.J. and Kingsman,S.M. (1994) *Nucleic Acids Res.*, **22**, 3365–3372.
- 20 Pearson,L., Chen,C.-h.B., Gaynor,R.P. and Sigman,D.S. (1994) *Nucleic Acids Res.*, **22**, 2255–2263.
- 21 White,A.S. and Draper,D.E. (1987) *Nucleic Acids Res.*, **15**, 4049–4064.
- 22 White,A.S. and Draper,D.E. (1989) *Biochemistry*, **28**, 1892–1897.
- 23 Battigello,J.-M.A., Cui,M., Roshong,S. and Carter,B.J. (1995) *Bioorg. Med. Chem.*, **3**, 839–849.